Metal−Metal Interactions as a Function of Bridging Ligand Topology: An Electrochemical, Spectroelectrochemical, and Magnetic Study on Dinuclear Oxo-Mo(V) Complexes with Various Isomers of Dihydroxynaphthalene as Bridging Ligand

Simon Bayly,[†] Jon A. McCleverty,*[,†] Michael D. Ward,*[,†] Dante Gatteschi,*[,‡] and Federico Totti[‡]

School of Chemistry, University of Bristol, Cantock's Close, Bristol BS8 1TS, U.K., and Department of Chemistry, University of Florence, Via Maragliano 75/77, 50144 Florence, Italy

Received October 22, 1999

Reaction of $[Mo^{V}(Tp^{Me,Me})(O)Cl_2]$ with 1,3-, 1,5-, 1,6-, 2,6-, and 2,7-dihydroxynaphthalene affords the dinuclear complexes $[\{Mo(Tp^{Me,Me})(O)Cl\}_2(\mu\text{-}C_{10}H_6O_2)]$, abbreviated as 1,3-**Mo**$_2$, 1,5-**Mo**$_2$, 1,6-**Mo**$_2$, 2,6-**Mo**$_2$, and 2,7-**Mo**$_2$, according to the substitution pattern of the bridging ligand. Electrochemical, UV−vis/NIR spectroscopic, and variable-temperature magnetic susceptibility studies have been used to probe the effects of the bridging-ligand topology on the metal−metal electronic and magnetic interactions. The complexes can be split into two classes according to the properties of the bridging ligands. Complexes 1,3-**Mo**$_2$, 1,6-**Mo**$_2$, and 2,7-**Mo**$_2$ all have bridging ligands that are topologically equivalent to meta-substituted bridging ligands such as 1,3-dihydroxybenzene, in that (i) there is an odd number of C atoms separating the two oxygen atoms, regardless of the pathway that is taken through the ligand skeleton, and (ii) the doubly oxidized form of the bridging ligand is a diradical. These complexes are classified as being "**T**-meta" (= topologically equivalent to meta). Complexes 1,5-**Mo**$_2$ and 2,6-**Mo**$_2$ have bridging ligands that are topologically equivalent to para-substituted groups such as 1,4-dihydroxybenzene, in that (i) there is an even number of C atoms separating the two oxygen atoms, whichever pathway is taken through the ligand skeleton, and (ii) the doubly oxidized form of the bridging ligand is a diamagnetic quinone. These complexes are classified as "**T**-para". Electrochemical studies show that the comproportionation constants for the Mo(V)/Mo(IV) mixed-valence states of the **T**-meta complexes are smaller than those for the **T**-para complexes. Spectroelectrochemical studies show that the Mo(V)/Mo(IV) mixed-valence states of the **T**-para complexes show pronounced Mo(IV)→Mo(V) IVCT transitions, whereas those of the **T**-meta complexes do not show these transitions. Magnetic susceptibility studies show that the **T**-meta complexes all display ferromagnetic exchange between the metal centers, whereas the **T**-para complexes all display antiferromagnetic exchange. Thus, both the electronic and the magnetic properties of these complexes show a clear demarcation into two sets according to the bridging-ligand topology.

Introduction

As part of our investigation into the electronic and magnetic interactions between metal centers across bridging ligands,[1,2] we have extensively studied dinuclear complexes of the $[\{Mo^{V}(Tp^{Me,Me})(O)Cl\}_2(\mu\text{-}\mathbf{OO})]$ type (in which $Tp^{Me,Me}$ is tris(3,5-dimethylpyrazolyl)hydroborate and **OO** denotes a deprotonated bis-phenolate type of bridging ligand with a 2^- charge).[1] This series of complexes has proven to be of particular interest for several reasons. First, the separation between the two successive oxidations [Mo(VI)/Mo(V) couples] and the two successive reductions [Mo(V)/Mo(IV) couples] provides an easy measurement of the extent of delocalization in the mixed-valence states as a function of the bridging ligand.[3] Second, spectroelectrochemical studies revealed the presence of remarkably intense transitions in the NIR region of the spectrum in the oxidized [Mo(V)−Mo(VI) and Mo(VI)−Mo(VI)] forms of the dinuclear complexes, ascribable to phenolate-to-Mo(VI) ligand-to-metal charge-transfer (LMCT) processes.[4] Third, the paramagnetism of the Mo(V) (d^1) fragment allowed measurement of the magnetic exchange interaction, *J*, as a function of the bridging ligand. In particular, for a series of dinuclear and trinuclear complexes, we demonstrated that the sign of *J* can be predicted using a simple spin-polarization scheme. For example, 1,4-$(OC_6H_4O)^{2-}$ affords antiferromagnetic coupling between the Mo(V) centers, whereas 1,3-$(OC_6H_4O)^{2-}$ affords ferromagnetic coupling.[5−7] Quantitative calculations at the DFT level have shown that the actual mechanism is more complex,[8] but nevertheless, the simple model, based on the alternating signs of induced spins along the bridging pathway, has a very useful

* Corresponding author. E-mail: mike.ward@bristol.ac.uk.
[†] University of Bristol.
[‡] University of Florence.

(1) McCleverty, J. A.; Ward, M. D. *Acc. Chem. Res.* **1998**, *31*, 842.
(2) Ward, M. D. *Chem. Soc. Rev.* **1995**, *24*, 121.
(3) Ung, V. A.; Bardwell, D. A.; Jeffery, J. C.; Maher, J. P.; McCleverty, J. A.; Ward, M. D.; Williamson, A. *Inorg. Chem.* **1996**, *35*, 5290.
(4) Harden, N. C.; Humphrey, E. R.; Jeffery, J. C.; Lee, S.-M.; Marcaccio, M.; McCleverty, J. A.; Rees, L. H.; Ward, M. D. *J. Chem. Soc., Dalton Trans.* **1999**, 2417.
(5) Ung, V. A.; Cargill Thompson, A. M. W.; Bardwell, D. A.; Gatteschi, D.; Jeffery, J. C.; McCleverty, J. A.; Totti, F.; Ward, M. D. *Inorg. Chem.* **1997**, *36*, 3447.
(6) Ung, V. A.; Couchman, S. M.; Jeffery, J. C.; McCleverty, J. A.; Ward, M. D.; Totti, F.; Gatteschi, D. *Inorg. Chem.* **1999**, *38*, 365.
(7) Cargill Thompson, A. M. W.; Gatteschi, D.; McCleverty, J. A.; Navas, J. A.; Rentschler, E.; Ward, M. D. *Inorg. Chem.* **1996**, *35*, 2701.
(8) Bencini, A.; Gatteschi, D.; Totti, F.; Sanz, D. N.; McCleverty, J. A.; Ward, M. D. *J. Phys. Chem. A* **1999**, *102*, 10 545.

10.1021/ic9912373 CCC: $19.00 © 2000 American Chemical Society
Published on Web 02/26/2000

Scheme 1[a]

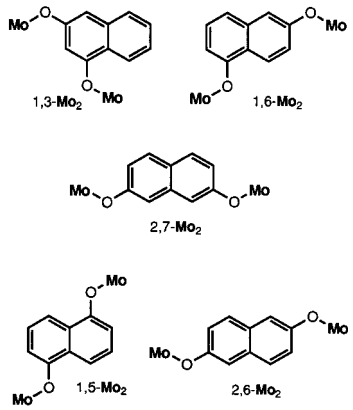

[a] **Mo** = {Mo(Tp^{Me,Me})(O)Cl}.

predictive value and is effective at predicting the sign of J in a wide range of dinuclear and trinuclear complexes.[5−7] Quite independently of each other, the electrochemical,[3] optical,[4] and magnetic[5,6] properties of these complexes have all proven to be noteworthy.

There have been many studies on the effects of ligand length on attenuating metal−metal interactions.[2,9] In these cases, however, the substitution pattern of the ligand (usually all para) does not change, as in the series pyrazine, 4,4′-bipyridine, 1,2-bis(4-pyridyl)ethene, and so forth. In contrast, the effects of changing the substitution pattern of aromatic bridging ligands have received relatively little attention. For example, it is well-known that meta-substituted aromatic bridging ligands are less effective at mediating electronic interactions than their para-substituted analogues;[2,10−12] however, beyond that, there has been little study of the effect. Similarly, apart from our recent work,[5−7] reports of the effects of changing the substitution pattern of the bridging ligand on the nature of the magnetic interaction between the metal centers are rare.[13]

In this paper, therefore, we address the effects of systematic variation in the substitution pattern of a planar dinucleating bridging ligand on both the electrochemical and magnetic interactions between two {Mo^{V}(Tp^{Me,Me})(O)Cl} fragments. It is worth emphasizing the particular value of the {Mo^{V}(Tp^{Me,Me})(O)Cl} fragment in this paper: being both redox active and paramagnetic, variations in electronic and magnetic interactions can be studied in parallel. The bridging ligands are various isomers of (doubly deprotonated) dihydroxynaphthalene, specifically, 1,3-, 1,5-, 1,6-, 2,6-, and 2,7-dihydroxynaphthalene. For our purposes, there are three particular advantages to this series of bridging ligands. First, as can be seen from Scheme 1, a wide variety of substitution patterns is available, in contrast to the more limited 1,2-, 1,3-, and 1,4-substitutions that are possible on a single aromatic ring. Therefore, we can extend the variation in ligand topology beyond the simple meta/para analogues. Second, in all cases, the bridging ligand is strictly planar, so there are no complications arising from changes in ligand conformation, in contrast to, for example, bridging ligands containing biphenyl[5] or bipyridyl[7] units. Third, the five dihydroxynaphthalene isomers used in this study are commercially available. We herein describe the preparation and characterization of the isomeric dinuclear complexes [{Mo(Tp^{Me,Me})(O)Cl}$_2$(μ-$C_{10}H_6O_2$)], hereafter abbreviated as 1,3-**Mo**$_2$, 1,5-**Mo**$_2$, 1,6-**Mo**$_2$, 2,6-**Mo**$_2$, and 2,7-**Mo**$_2$ according to the substitution pattern of the bridging ligand (Scheme 1) and their magnetic, electrochemical, and spectroelectrochemical properties.

Table 1. Experimental and Analytical Data for the New Complexes

complex	reaction time (h)	yield (%)	analysis[a] %C	%H	%N	FAB-MS[b] (m/z)
1,3-**Mo**$_2$	3.5	50	46.8 (45.9)	5.3 (4.8)	15.7 (16.0)	1048
1,5-**Mo**$_2$	0.75	42	45.2 (45.9)	5.1 (4.8)	15.3 (16.0)	1047
1,6-**Mo**$_2$	0.5	56	46.3 (45.9)	4.3 (4.8)	15.4 (16.0)	1046
2,6-**Mo**$_2$	0.75	38	43.0 (43.5)[c]	5.0 (4.6)	14.7 (14.8)	1048
2,7-**Mo**$_2$	1.75	57	48.6 (48.7)[d]	6.1 (5.7)	14.4 (14.8)	1046

[a] Calculated values in parentheses. [b] 3-Nitrobenzyl alcohol matrix; the most intense peak of the isotope cluster should occur at m/z = 1047 in every case. [c] One molecule of CH_2Cl_2 per complex molecule is assumed for the elemental analysis. [d] One molecule of hexane per complex molecule is assumed for the elemental analysis.

Results and Discussion

Complex Syntheses. The complexes were readily prepared by reaction of 2 equiv of [Mo(Tp^{Me,Me})(O)Cl$_2$][14] with 1 equiv of the appropriate dihydroxynaphthalene in toluene at reflux, in the presence of Et_3N. However, one important variation from the standard synthetic method for previous complexes of this type is that simple mixing of the metal precursor with the bridging ligand and the base, followed by prolonged reflux, afforded only very small yields of the dinuclear complexes. We ascribe this to the insolubility of the dihydroxynaphthalene isomers in toluene. Much better yields were obtained by first treating the dihydroxynaphthalene with Et_3N in toluene at reflux, followed by the subsequent addition of the metal reagent, which then coordinated very quickly. Following chromatographic purification of the complexes, satisfactory elemental analyses and FAB mass spectra were obtained in all cases (Table 1).

Topological Properties of the Bridging Ligands. The bridging ligands can be split into two sets, according to whether it is possible to draw a quinone for the doubly oxidized form. A simple illustration of this is provided by a comparison of the deprotonated dianions of 1,3-dihydroxybenzene and 1,4-dihydroxybenzene. In the former case, two-electron oxidation results in a ferromagnetically coupled diradical[15−18] because there are two degenerate frontier orbitals, spatially coextensive but symmetrically orthogonal, that accommodate one electron each.[19] These properties are associated with an odd number of carbon atoms that separate the oxygen atoms either way around the ring. In 1,4-$[C_6H_4O_2]^{2-}$, however, two-electron oxidation results in a diamagnetic quinone because the unpaired electrons that arise on the oxygen atoms on oxidation can pair up in a single orbital; this is associated with an even number of carbon atoms along the pathway between the oxygen atoms. Although both molecules have even-alternant structures, the 1,3-isomer is representative of the subgroup that can form non-Kekulé structures (a diradical), whereas the 1,4-isomer is representative

(9) Ribou, A.-C.; Launay, J.-P.; Sachtleben, M. L.; Li, H.; Spangler, C. W. *Inorg. Chem.* **1996**, *35*, 3575.
(10) Wlodarczyk, A.; Maher, J. P.; McCleverty, J. A.; Ward, M. D. *J. Chem. Soc., Chem. Commun.* **1995**, 2397.
(11) Richardson, D. E.; Taube, H. *J. Am. Chem. Soc.* **1983**, *105*, 40.
(12) Karafiloglou, P.; Launay, J.-P. *J. Phys. Chem. A* **1998**, *102*, 8004.
(13) Lloret, F.; De Munno, G.; Julve, M.; Cano, J.; Ruiz, R.; Caneschi, A. *Angew. Chem., Int. Ed. Engl.* **1998**, *37*, 135.
(14) Cleland, W. E., Jr.; Barhhart, K. M.; Yamanouchi, K.; Collison, D.; Mabbs, F. E.; Ortega, R. B.; Enemark, J. H. *Inorg. Chem.* **1987**, *26*, 1017.
(15) Miller, J. S.; Epstein, A. J. *Angew. Chem., Int. Ed. Engl.* **1994**, *33*, 385.
(16) Rajca, S. *Chem. Rev.* **1994**, *94*, 871.
(17) Yoshizawa, K.; Hoffman, R. *Chem.−Eur. J.* **1995**, *1*, 403.
(18) Iwamura, H.; Koga, N. *Acc. Chem. Res.* **1993**, *26*, 346.
(19) Longuet-Higgins, J. C. *J. Chem. Phys.* **1950**, *18*, 265.

Table 2. Electrochemical Data[a]

	$E_{1/2}$, Volts vs ferrocene/ferrocenium					
complex	Mo(V)/Mo(IV) couples		E, mV	Mo(VI)/Mo(V) couples		ΔE, mV
1,3-**Mo**$_2$	−1.22	−1.42	200	+0.36 (i)[b]		
1,5-**Mo**$_2$	−1.24	−1.39	150	+0.34	+1.01 (i)	670
1,6-**Mo**$_2$	−1.17	−1.29	120	+0.45 (i)		
2,6-**Mo**$_2$	−1.24	−1.38	140	+0.26	+1.04 (i)	780
2,7-**Mo**$_2$	−1.17	−1.29	120	+0.53 (i)		

[a] All measurements made in CH_2Cl_2 containing 0.1−0.2 M Bu_4NPF_6, using Pt-bead working and counter electrodes and an SCE reference electrode. Ferrocene was added at the end of each experiment as an internal reference, and all potentials are quoted vs the ferrocene/ferrocenium couple. Half-wave potentials were checked by both cyclic and square-wave voltammetry. All processes are chemically reversible except where explicity stated otherwise. [b] (i) = irreversible; the peak potential was measured from the square-wave voltammogram.

of the other subgroup for which a diamagnetic Kekulé-type structure exists.[20]

This same principle can be extended to the dihydroxynaphthalenes used here. Simple inspection shows that the 1,3-, 1,6-, and 2,7-dihydroxynaphthalene isomers can be grouped with 1,3-dihydroxybenzene as bridging ligands, insofar as there is always an odd number of carbon atoms separating the oxygen atoms, regardless of whichever pathway is followed around the naphthyl skeleton. For convenience, we define these ligands (and others with the same property) as "**T**-meta", meaning topologically similar to a meta-substituted ligand. We therefore expect these bridging ligands (i) to give ferromagnetic coupling between paramagnetic metal complex fragments coordinated to the oxygen atoms on the basis of spin-polarization[5−7,13,21−23] and (ii) to give weaker electrochemical interactions between the metal centers. Conversely, the 1,5- and 2,6-dihydroxynaphthalene isomers can be grouped with 1,4-dihydroxybenzene, in that there is always an even number of carbon atoms separating the oxygen atoms, regardless of the pathway that is followed around the naphthyl skeleton. These ligands are collectively denoted "**T**-para" (topologically similar to a para-substituted bridging ligand) and are therefore expected to give (i) antiferromagnetic coupling and (ii) stronger electrochemical interactions between the metal centers.

Electrochemical Properties. Redox potentials for all of the complexes, measured from cyclic and square-wave voltammetry, are summarized in Table 2. All five complexes undergo two reversible one-electron reductions, which are successive Mo(V)/Mo(IV) couples. This behavior is an agreement with the earlier dinuclear complexes of this type,[3] although the planarity and the relatively short metal−metal separations of these dihydroxynaphthalene-bridged complexes, compared to the polyphenylene-bridged complexes we examined earlier, result in greater redox separations ($\Delta E_{1/2}$). The separation of 200 mV between the reductions in 1,3-**Mo**$_2$ is identical to that which was observed in [{Mo(Tp^{Me,Me})(O)Cl}$_2$(μ-1,3-OC$_6$H$_4$O)], in which the bridging ligand is deprotonated 1,3-dihydroxybenzene. In the other four complexes, for which the metal−metal separation is greater because the two metal fragments are attached to different rings of the bridging ligand, the redox separations between the two Mo(V)/Mo(IV) couples are significantly smaller but similar to one another (120−150 mV). However, the redox splittings in the two **T**-para isomers 1,5-**Mo**$_2$ (150 mV) and 2,6-**Mo**$_2$ (140 mV) are greater than those of the **T**-meta isomers 1,6-**Mo**$_2$ and 2,7-**Mo**$_2$ (120 mV each), which is as expected on the basis of the topological considerations described in the previous section, although the effect is not large.

A similar effect of the bridging ligand topology on the redox properties can be seen in the oxidative behavior of these new complexes. The **T**-para 1,5-**Mo**$_2$ and 2,6-**Mo**$_2$ isomers show two oxidations, separated by 670 and 780 mV, respectively; only the first is fully reversible in each case. This is similar to the behavior of [{Mo(Tp^{Me,Me})(O)Cl}$_2$(μ-1,4-OC$_6$H$_4$O)], which showed a 990 mV separation between the two oxidations, the second of which was irreversible. In contrast, the **T**-meta isomers 1,3-**Mo**$_2$, 1,6-**Mo**$_2$, and 2,7-**Mo**$_2$ all show only a single irreversible oxidation, which is exactly like the behavior of [{Mo(Tp^{Me,Me})(O)Cl}$_2$(μ-1,3-OC$_6$H$_4$O)].[3]

The origin of this difference in electrochemical behavior for the two classes of complex is not obvious. We originally thought that the oxidations could be ligand-centered,[3] with the para-substituted complexes undergoing two such oxidations to give a bridging quinone but the meta-substituted complexes giving an unstable ligand-centered radical that decomposed. This explanation is certainly consistent with the behavior we see here. However, recent ZINDO calculations and spectroelectrochemical studies on representative dinuclear complexes suggested that the oxidations are predominantly metal-centered Mo(V)/Mo(VI) couples,[4] which does not explain why variation of the bridging ligand has such a profound effect on the electrochemical behavior. The most likely explanation is that, although the oxidations are best described as formally metal-centered Mo(V)/Mo(VI) couples,[4] they are partly delocalized onto the bridging ligand via a suitable π-symmetry orbital. There is, therefore, sufficient ligand-centered character to the oxidations that the number and reversibility of these processes is affected by whether the bridging ligand can give a stable quinone on oxidation. Thus, following oxidation of (say) 1,3-**Mo**$_2$, the formally mixed-valence Mo(V)/Mo(VI) species will have a small admixture of the canonical form in which both metals are in oxidation state +5, but the ligand is now an unstable radical, which provides a facile decomposition pathway. In the same way, highly extended quinones can be unstable because of a slight admixture of diradical character from an alternative canonical form (that is, a low-energy excited state), which provides a decomposition pathway, despite making a very small contribution to the structure.[24,25]

UV−Vis/NIR Spectroelectrochemical Properties. We performed spectroelectrochemical studies on these complexes in all oxidation states that were accessible by fully reversible processes: viz. the mono- and direduced Mo(V)/Mo(IV) and Mo(IV)/Mo(IV) states for all five complexes and the mono-oxidized Mo(V)/Mo(VI) states for 1,5-**Mo**$_2$ and 2,6-**Mo**$_2$. The results are collected in Table 3; see also Figures 1 and 2.

The spectra recorded during successive reductions of the **T**-meta isomers 1,3-**Mo**$_2$, 1,6-**Mo**$_2$, and 2,7-**Mo**$_2$ from the Mo(V)/Mo(V) state to the Mo(V)/Mo(IV) and then Mo(IV)/Mo(IV) states follow the pattern that we have seen before for [{Mo(Tp^{Me,Me})(O)Cl}$_2$(μ-1,3-OC$_6$H$_4$O)].[4] The most important point is that the phenolate→Mo(V) LMCT transition, which lies between 600 and 700 nm, approximately halves in intensity on the first reduction and is slightly red-shifted; the second

(20) Ollis, W. D.; Stanforth, S. P.; Ramsden, C. A. *Tetrahedron* **1985**, *41*, 2239.
(21) Karafiloglou, P. *J. Chem. Phys.* **1985**, *82*, 3728.
(22) Ovchinnikov, A. A. *Theor. Chim. Acta* **1978**, *47*, 297.
(23) Rajca, A.; Rajca, S. *J. Am. Chem. Soc.* **1996**, *118*, 8121.
(24) Dimroth, K.; Umbach, W.; Blöcher, K. H. *Angew. Chem., Int. Ed. Engl.* **1963**, *2*, 620.
(25) Bourdon, J.; Calvin, M. *J. Org. Chem.* **1957**, *22*, 101.

Table 3. UV−VIS/NIR Spectroscopic Data for the Complexes in all Accessible Oxidation States[a]

complex	ox states[b]	λ_{max}, nm [$10^{-3}\epsilon$, M^{-1} cm^{-1}]					
1,3-**Mo**$_2$	5,5	665 (3.7)[c]	410 (sh)	300 (sh)			
	5,4	732 (2.2)[c]	440 (sh)	318 (12)			
	4,4	830 (0.3)[d]	435 (sh)	370 (sh)	342 (9.3)		
1,5-**Mo**$_2$	6,5	1304 (13)[e]	1112 (8.5)[e]	970 (sh)[e]	583 (7.3)[e]	350 (sh)	275 (15)
	5,5	691 (4.2)[c]	420 (7.2)	307 (sh)	279 (18)		
	5,4	1250 (sh)[f]	756 (2.2)[c]	428 (sh)	360 (sh)	325 (11)	
	4,4	830 (0.4)[d]	389 (11)	330 (sh)			
1,6-**Mo**$_2$	5,5	650 (3.1)[c]	410 (sh)	306 (14)	270 (sh)		
	5,4	708 (1.5)[c]	447 (sh)	368 (sh)	315 (11)	255 (sh)	
	4,4	810 (0.3)[d]	440 (sh)	364 (8.1)	323 (10)	261 (18)	
2,6-**Mo**$_2$	6,5	958 (11)[e]	617 (9.7)[e]	449 (3.7)	286 (sh)		
	5,5	677 (3.9)[c]	411 (6.0)	265 (16)			
	5,4	1150 (0.9)[f]	737 (2.1)[c]	426 (3.2)	363 (sh)	305 (8.2)	
	4,4	750 (0.6)[d]	368 (6.2)	315 (7.0)	270 (12)		
2,7-**Mo**$_2$	5,5	608 (3.7)[c]	360 (11)	266 (sh)			
	5,4	615 (2.1)[c]	276 (sh)				
	4,4	820 (0.7)[d]	430 (sh)	375 (sh)	304 (19)		

[a] All spectra recorded at −30 °C in CH_2Cl_2. [b] This column denotes the metal oxidation states: thus (5,5) is the Mo(V)/Mo(V) complex before any electrolysis; (5,4) is the Mo(V)/Mo(IV) mixed-valence state, and so on. [c] Phenolate→Mo(V) LMCT. [d] Mo(IV)-centered d−d transition (see ref 4). [e] Phenolate→Mo(VI) LMCT (see ref 4). [f] Mo(IV)→Mo(V) IVCT.

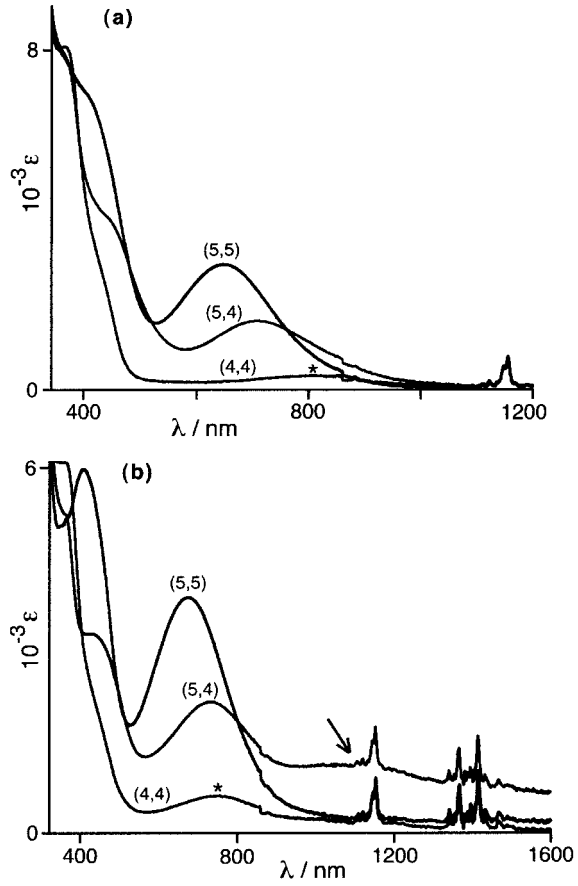

Figure 1. Electronic spectra of (a) 1,6-**Mo**$_2$ and (b) 2,6-**Mo**$_2$ in oxidation states Mo(V)/Mo(V), Mo(V)/Mo(IV), and Mo(IV)/Mo(IV). The Mo(IV)-centered weak d−d transition is marked with an asterisk (*) in each case. The IVCT transition in the Mo(V)/Mo(IV) state of 2,6-**Mo**$_2$ is shown by the arrow in (b). The sharp spikes at wavelengths longer than 1000 nm are IR overtones from the solvent.

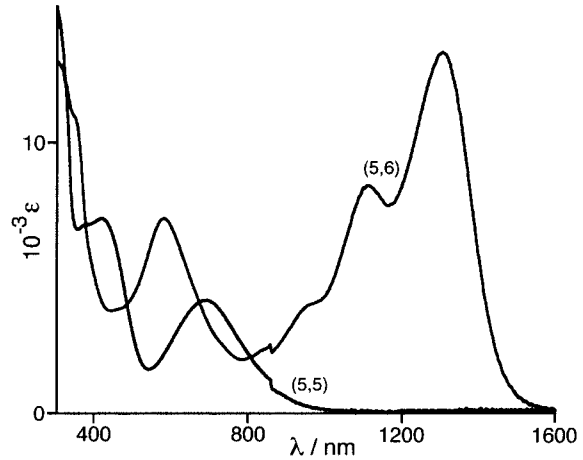

Figure 2. Electronic spectrum of 1,5-**Mo**$_2$ in the Mo(V)/Mo(V) and Mo(V)/Mo(VI) oxidation states, showing the strong near-IR absorbance in the oxidized form of the complex.

reduction makes it disappear completely (Figure 1a). This occurs because the vacancies in the d_{xy} orbitals on both metals, which act as the recipients for the phenolate→Mo(V) LMCT transitions, become filled such that this transition can no longer occur. This behavior is entirely consistent with that expected from the two fragments that are at most weakly interacting. In the fully reduced Mo(IV)/Mo(IV) state, there is a weak transition at ∼800 nm in each case, which is a d−d transition within the d(π) manifold (formally d_{xy}→d_{xz}/d_{yz}, assuming that the Mo=O bond is on the *z*-axis),[1] arising because of the substantial splitting of these three orbitals results in a low-spin d_{xy}^2 configuration for the Mo(IV) oxidation state.[4]

The **T**-para isomers 1,5-**Mo**$_2$ and 2,6-**Mo**$_2$ behave similarly, in that the phenolate→Mo(V) LMCT transition disappears on reduction. However, their behavior is significantly different to that of the **T**-meta isomers in that in the mixed-valence Mo(V)/Mo(IV) state an additional, moderately intense ($\epsilon \approx 1000$ M^{-1} cm^{-1}) new transition appears in the NIR region (∼1250 nm for 1,5-**Mo**$_2$ and ∼1150 nm for 2,6-**Mo**$_2$; see Figure 1b). The exact wavelengths are difficult to determine as these transitions are broad and appear as shoulders on the low-energy side of the phenolate→Mo(V) LMCT transition. We ascribe this new transition in each case to a Mo(IV)→Mo(V) intervalence charge-transfer (IVCT) process, which is now permitted because of the improved delocalization between the metal centers afforded by the **T**-para structures of these bridging ligands. On further reduction to the Mo(IV)/Mo(IV) state, this IVCT transition disappears in each case. IVCT transitions in this region of the spectrum were likewise observed in the Mo(V)/Mo(IV) state of [{Mo($Tp^{Me,Me}$)(O)Cl}$_2$(μ-1,4-OC_6H_4O)],[4] and it is clear that the 1,5- and 2,6-dihydroxynaphthalene dianions share the ability

of 1,4-$[OC_6H_4O]^{2-}$ to act as an effective mediator of electron-transfer between the metal centers because of their related topological properties. The intensities of the IVCT transitions, and the rather modest redox separations for the two Mo(V)/Mo(IV) couples in each case, suggest that the mixed-valence states are best described as class II in the Robin−Day classification.

The oxidation of 2,6-**Mo**$_2$ by one electron to the mixed-valence Mo(V)/Mo(VI) state results in the replacement of the phenolate→Mo(V) LMCT transition by two intense new transitions, one at slightly higher energy (617 nm) and one at lower energy in the NIR region (958 nm). This behavior is consistent with our previous observations on complexes of this type, with the two transitions being ascribed to phenolate→Mo(VI) LMCT transitions to the two distinct sets of d(π) orbitals (d_{xy} being lower in energy than d_{xz}/d_{yz} which are approximately degenerate).[4] Oxidation of 1,5-**Mo**$_2$ by one electron results in similar spectroscopic changes, with the important difference being that the lower energy (NIR) transition is at much lower energy (λ_{max} = 1304 nm) and additional weaker transitions on the high-energy side are also resolved at 1112 and 970 nm (Figure 2, Table 3); the constant spacing of ~1320 cm^{-1} in this series suggests that it is a vibrational progression, although without knowing the IR spectrum of the oxidized form of the complex, we cannot say which vibrational mode is involved. The lower energy of this LMCT transition for 1,5-**Mo**$_2$, compared to 2,6-**Mo**$_2$, suggests that its bridging-ligand centered HOMO is higher in energy, a fact which was supported by a simple extended-Hückel calculation on the deprotonated dianions (HOMO for 1,5-$[C_{10}H_8O_2]^{2-}$, −10.9 eV; HOMO for 2,6-$[C_{10}H_8O_2]^{2-}$, −11.2 eV).

Materials that show a very strong absorbance in the NIR region of the spectrum are of technological interest as dyes for numerous applications that rely on NIR lasers.[26−28] If the absorbance is not permanent, but may be switched on and off electrochemically, then the material is said to be electrochromic and is of interest for examples like electrooptic switching.[29,30] We have recently prepared a wide variety of complexes that show very pronounced NIR electrochromism,[4,31−33] and the behavior of 1,5-**Mo**$_2$ in particular is a significant addition to this field.

Magnetic Properties. In addition to the variation of electronic interactions according to the topology of the bridging ligand, we also expect the magnetic interactions between the paramagnetic Mo(V) centers to be modulated in the same way. On the basis of the spin-polarization picture, which has worked reliably for other complexes in this series,[5−7] we expect the **T**-meta bridging ligands to afford ferromagnetic coupling and the **T**-para bridging ligands to afford antiferromagnetic coupling.

The results of variable-temperature magnetic susceptibility measurements on the complexes are collected in Table 4 (see also Figure 3). The fits of the variable-temperature magnetic susceptibility data in the temperature range 1.6−250 K were used to determine the values of J, the exchange coupling constant between each pair of metal ions, using the exchange spin Hamiltonian in the form $H = -J$ **(S_1S_2)**, with positive J indicating ferromagnetism and negative J indicating antiferromagnetism.

Table 4. Magnetic Parameters for the Complexes Derived from Susceptibility Measurements[a]

	1,3-**Mo**$_2$	1,5-**Mo**$_2$	1,6-**Mo**$_2$	2,6-**Mo**$_2$	2,7-**Mo**$_2$
g	1.913(1)	1.90(1)	1.908(9)	1.90	1.92(4)
J (cm^{-1})	28.7(6)	−10.10(8)	17.4	−28.5	12(1)
ρ				4.7%	
TIP (cm^3 mol^{-1})				0.0017	
CFA[b] (cm^{-1} molecule)	0.1		0.14(1)		0.1(7)

[a] Errors are reported in parentheses where appropriate; where no error is given, a trial-and-error approach has been used. [b] Acronym for crystal field approximation; see ref 35.

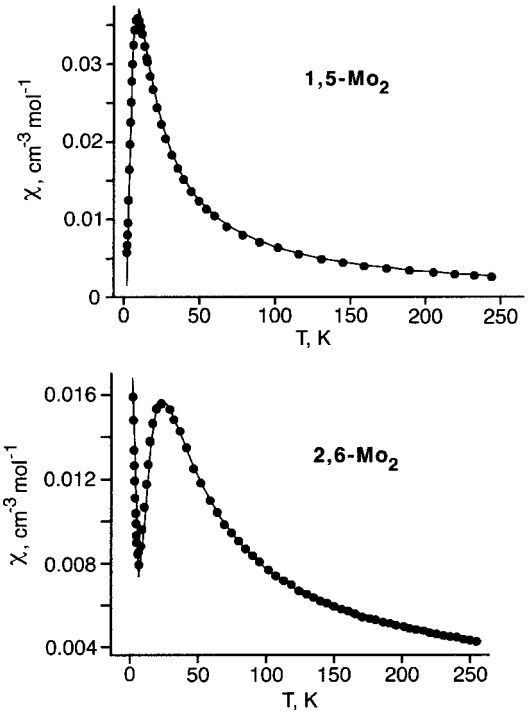

Figure 3. Magnetic susceptibility data for 1,5-**Mo**$_2$ and 2,6-**Mo**$_2$.

The group of **T**-meta complexes 1,3-**Mo**$_2$, 1,6-**Mo**$_2$, and 2,7-**Mo**$_2$ all display ferromagnetic exchange with J values of +28.7, +17.4, and +12 cm^{-1}, respectively. That the first of these is the largest is not surprising, as in 1,3-**Mo**$_2$ alone, the two **Mo** fragments are attached to the same aromatic ring, and this value may be compared with J = +9.8 cm^{-1} for the ferromagnetic coupling in [{Mo(Tp^{Me,Me})(O)Cl}$_2$(μ-1,3-OC_6H_4O)] across the 1,3-substituted bridging ligand. 1,3-Dihydroxynaphthalene is, in this case, clearly a more effective "ferromagnetic coupling unit" than 1,3-dihydroxybenzene. The higher effectiveness of the naphthalene compared to the benzene skeleton at mediating magnetic exchange in these complexes is confirmed by the fact that the three coupling constants reported here are all larger than that of 1,3-dihydroxybenzene, despite the greater metal−metal separation in two of the cases (1,6-**Mo**$_2$ and 2,7-**Mo**$_2$). It is certainly interesting to notice that sizable ferromagnetic coupling can be established between two Mo(V) centers which are ~10 Å apart (in 2,7-**Mo**$_2$, the Mo···Mo separation being estimated on the basis of molecular modeling studies).

Conversely, the **T**-para complexes 1,5-**Mo**$_2$ and 2,6-**Mo**$_2$ are antiferromagnetically coupled (J = −9.6 and −28.3 cm^{-1} respectively), but in these cases, the coupling is lower than

(26) Emmelius, M.; Pawlowski, G.; Vollmann, H. W. *Angew. Chem., Int. Ed. Engl.* **1989**, *28*, 1445.
(27) Fabian, J.; Zahradnik, R. *Angew. Chem., Int. Ed. Engl.* **1989**, *28*, 677.
(28) Fabian, J.; Nakazumi, H.; Matsuoka, M. *Chem. Rev.* **1992**, *92*, 1197.
(29) Mortimer, R. J. *Chem. Soc. Rev.* **1997**, *26*, 147.
(30) Mortimer, R. J. *Electrochim. Acta* **1999**, *44*, 2971.
(31) Barthram, A. M.; Cleary, R. L.; Kowallick, R.; Ward, M. D. *Chem. Commun.* **1998**, 2695.
(32) Lee, S.-M.; Marcaccio, M.; McCleverty, J. A.; Ward, M. D. *Chem. Mater.* **1998**, *10*, 3272.
(33) Kowallick, R.; Jones, A. N.; Reeves, Z. R.; Jeffery, J. C.; McCleverty, J. A.; Ward, M. D. *New J. Chem.* **1999**, *23*, 915.

observed for the 1,4-dihydroxybenzene-bridging complex ($J = -80$ cm^{-1}) in part because the metal atoms are attached to different aromatic rings. The different values of J for 1,5-**Mo**$_2$ and 2,6-**Mo**$_2$, which have comparable metal−metal separations, cannot be easily rationalized in terms of differences in the magnetic pathways; for example, the shortest through-bond pathway between the metal centers in 1,5-**Mo**$_2$ is shorter than that in 2,6-**Mo**$_2$ and yet gives a weaker magnetic exchange. However, it is again noteworthy that a coupling constant of -28.3 cm^{-1} is observed for a metal−metal distance of ∼10 Å (estimated from molecular modeling studies). The fact that 1,5- and 2,6-dihydroxynaphthalene both promote antiferromagnetic exchange is in agreement with their topological similarity to 1,4-dihydroxybenzene, which was also apparent from the spectroelectrochemical studies.

Conclusions

It has long been known that para-substituted aromatic bridging ligands are more effective than their meta-substituted analogues at facilitating metal−metal interactions. In this paper, we have shown that the same principle can be extended to more complex polycyclic aromatic bridging ligands which are topologically related to the simpler monocyclic meta- and para-substituted analogues. Thus the **T**-para class of bridging ligands all allow stronger electronic interactions between the metal fragments than the **T**-meta class, as shown by (i) the electrochemical properties of the complexes and (ii) the presence or absence of IVCT bands in the spectra of the mixed-valence forms. The magnetic exchange interactions likewise conform to this principle, with the **T**-para class of bridging ligands all acting as antiferromagnetic linking units but the **T**-para bridging ligands acting as ferromagnetic linking units.

Experimental Section

General Details. The instrumentation used for routine spectroscopic and electrochemical studies has been recently described.[34] Spectroelectrochemical studies were performed in CH_2Cl_2 solution at −30 °C using a home-built OTTLE cell mounted in the sample compartment of a Perkin−Elmer Lambda 19 spectrophotometer, as described previously;[34] the chemical reversibility of each process was checked by reversing the applied potential after electrolysis and ensuring that the spectrum of the starting material could be regenerated. Magnetic susceptibilities were measured in the temperature range of 1.6−250 K in an applied field of 1 T using a Metronique Ingéniérie MS03 SQUID magnetometer; diamagnetic corrections were estimated from Pascal's constants.[35,36] The values of the parameters obtained by the fitting procedure are reported in Table 1. [Mo(Tp^{Me,Me})(O)Cl$_2$] was prepared according to the method of Enemark et al.[14] The various isomers of dihydroxynaphthalene were obtained from the usual commercial sources (Aldrich, Lancaster) and used as received.

Preparations of Complexes. The same method was used for all five complexes. A mixture of the appropriate dihydroxynaphthalene (0.080 g, 0.5 mmol) and excess Et_3N in dry toluene was heated to reflux for 1 h under N_2. After this time, [Mo(Tp^{Me,Me})(O)Cl$_2$] (0.48 g, 1.0 mmol) was added, and the mixture was maintained at reflux. The reaction was followed by thin-layer chromatography (silica, CH_2Cl_2) until no further change occurred (see Table 1 for reaction times). After the mixture was cooled and the solvent was removed in vacuo, the crude mixture was purified by column chromatography (silica, CH_2Cl_2), with the principal dark-green band being collected in each case. Yield and characterization data for the complexes are collected in Table 1.

Acknowledgment. We thank the EPSRC (UK) for a Ph.D. studentship (to S.B.).

IC9912373

(34) Lee, S.-M.; Kowallick, R.; Marcaccio, M.; McCleverty, J. A.; Ward, M. D. *J. Chem. Soc., Dalton Trans.* **1998**, 3443.
(35) O'Connor, C. J. *Prog. Inorg. Chem.* **1982**, *29*, 203.
(36) Carlin, R. L. *Magnetochemistry*; Springer-Verlag: New York, 1986.